IEEE Access
Multidisciplinary | Rapid Review | Open Access Journal

Received June 24, 2019, accepted July 5, 2019, date of publication July 9, 2019, date of current version August 9, 2019.

Digital Object Identifier 10.1109/ACCESS.2019.2927753

Performance Analysis of Nonlinear SFBC OFDM Systems Over TWDP Fading Channel

YIPENG DU[1], (Student Member, IEEE), JIAN LIU[2], (Member, IEEE), AND YUAN CHEN[2], (Member, IEEE)

[1]School of Electronics Engineering and Computer Science, Peking University, Beijing 100871, China
[2]School of Computer and Communication Engineering, University of Science and Technology Beijing, Beijing 100083, China

Corresponding author: Yipeng Du (duyp@pku.edu.cn)

This work was supported in part by the 2018 Sugon Intelligent-Factory on Advanced Computing Devices under Grant MIIT2018-265-137, and in part by the National Natural Science Foundation of China under Grant 61701021.

ABSTRACT In this paper, the practical performance of space-frequency block code (SFBC)-based multiple-input multiple-output (MIMO) orthogonal frequency division multiplexing (OFDM) system in the presence of nonlinear power amplifier with imperfect channel state information (CSI) over two-wave with diffuse power (TWDP) channel is analyzed. In the performance analysis, we first introduce the equivalent single-input single-output (SISO) scalar model with nonlinear power amplifier and then the SISO model is used to construct a model for the nonlinear MIMO-OFDM system. Considering the channel estimation error at the receiver, we study the effects of MMSE channel estimation error on the channel capacity. What is more, based on inter modulation product (IMP) analysis, we study the BER performance of nonlinear SFBC MIMO-OFDM systems, considering M-ary phase shift keying (MPSK) and M-ary quadrature amplitude modulation (MQAM). And the effects of channel estimation error on the BER performance are studied. Finally, this paper also derives the closed-form expressions of the system optimal operating point. The numerical results and comparisons are provided for several forms of SFBC MIMO-OFDM. From these analysis results, it is found that the analytical interpretation of the observed behavior in the simulation can be advanced, and the actual analysis of the performance optimization of the nonlinear MIMO-OFDM system is also provided.

INDEX TERMS BER, channel estimate error, MMSE, MIMO-OFDM, nonlinear PA, SFBC.

I. INTRODUCTION

Orthogonal Frequency Division Multiplexing (OFDM) is widely used as an attractive technology in modern wireless communications due to its robustness to frequency selective fading channels and its potential to achieve high data rates [1]. In order to meet the explosive growth requirements of mobile data access, various multiple-input multiple-output OFDM (MIMO-OFDM) schemes with space-frequency block coding (SFBC) have been used for long-term evolution - advanced (LTE-A) Standard [2], [3]. In addition, MIMO is generally considered to be a supporting technology for the development of fifth-generation (5G) broadband mobile networks. When MIMO technology is introduced into an OFDM-based system, spectral efficiency and energy efficiency are improved.

In recent works, the performance of SFBC-OFDM systems was studied using numerical analysis. In [4], they propose a novel algorithm to identify SFBC by analyzing discriminating features for different SFBC. In [5], they develop and analyze an SFBC identification algorithm for multiple antenna OFDM transmission for the first time. An integer carrier frequency offset (CFO) estimation algorithm for a SFBC system is proposed in [6]. A cooperative single-carrier transmission scheme considering a distributed quasi-orthogonal space-frequency block code (QOSFBC) is constructed in [7]. Several novel peak-to-average power ratio (PAPR) reduction schemes are proposed for SFBC MIMO-OFDM system in [8] and [9]. In [10], they have designed Alamouti-like space-time block coded (STBC) and space-frequency block coded vector OFDM system. Moreover, an iterative pilot-aided channel estimation technique for SFBC MIMO-OFDM systems is proposed in [11]. Furthermore, BER analysis of SFBC-OFDM systems under different fading conditions has been reported in the literature [12]–[16]. In [12], the frame error rate and outage probability for STBC and SFBC OFDM systems for BPSK and QPSK modulation are given.

The associate editor coordinating the review of this manuscript and approving it for publication was Qingchun Chen.

A closed-form expression of the BER of the SFBC OFDM system based on MQAM and MPSK is derived in [13]. Later, Singh et al. conducted an in-depth study of performance of SFBC-OFDM over different fading channels with channel estimation error [14]–[16].

But SFBC-OFDM systems have a major weakness, i.e., the significant nonlinear distortion caused by power amplifiers, [17]. To study the above indicative papers, it is worth noting that the analysis of SFBC-OFDM with nonlinear power amplifier under imperfect channel state information (CSI), also called nonlinear SFBC-OFDM, is lacked. Is the equivalent SISO scalar model effective for SFBC MIMO-OFDM systems when considering clear nonlinear distortion that power amplifier (PA) produces and the imperfections on the CSI? How does channel estimation error and PA nonlinear distortion affect the channel capacity of SFBC MIMO-OFDM? Is the relationship between receiver signal-to-noise ratio (SNR) and PA operating point relatively convenient at different channel estimation error levels? Is there any asymptotic behavior of SNR and any analytical expression of the best PA operating point corresponding to the maximum SNR? Given the nonlinear distortion at the receiver, is there an expression for the bit error rate of MPSK and MQAM modulated signals?

The main purpose of this paper is to explore the practical performance analysis of SFBC MIMO-OFDM system in the nonlinear noise generated by the power amplifier under imperfect CSI. In order to simulate the channel environment of the real scene, we study the nonlinear SFBC-OFDM system over two-wave with diffuse power (TWDP) fading channel. In this paper, we apply the SISO scalar model to the studied nonlinear SFBC MIMO systems to simplify the complexity of the analysis. For the channel estimation error, we consider the effects of MMSE. Specifically, we study the lower and upper bounds of mutual information and channel capacity with a channel estimate at the receiver and perfect feedback. For the BER analysis, we derive closed-form expressions for nonlinear SFBC MIMO-OFDM systems over TWDP fading channels, and both MPSK and MQAM are considered. Moreover, we model the inter modulation product falling (IMP) as a Gaussian signal and the inter modulation product analysis is combined with the accurate Bessel-Fourier PA model. From these derivations above, we derive the optimal system operating point to a polynomial based expression, and it corresponds to the BER lower bound. In addition, the channel estimation error reduces the system performance of SFBC MIMO-OFDM system. The total degradation (TD) performance is investigated as well. These simulation observations are explained by the derivation proposed in this paper.

The rest of this paper is organized as follows. In Section II, the SFBC MIMO-OFDM system is considered when nonlinear distortion and channel estimation error are considered. In Section III, lower and upper bounds of mutual information for nonlinear SFBC MIMO-OFDM under imperfect CSI are derived. And the capacity bounds are also derived. The BER expressions for PSK and QAM signals based expression of receiver SNR with nonlinear noise and channel estimation error are derived in section IV. In section V, we derive the accurate expression of the best system operating point. In the Section VI, simulated observations are presented and analytical interpretations are performed. Next is the conclusion of Section VII.

In this paper, $(.)^T$ indicates the transposition of the matrix, and $\mathbf{A}$(i,j) represents the element of the i^{th} row and j^{th} column of the matrix $\mathbf{A}$. $E(.)$ expresses expectations of the matrix. $Nd(0, 1)$ represents a Gaussian distribution with a mean of 0 and a variance of 1.

II. SYSTEM MODEL

Fig.1 shows a basic model of SFBC MIMO-OFDM system with X_T transmit and X_R receive antennas. For the convenience of expression, we define that OFDM system has B subcarriers. The $B_t \times 1$ matrix $\mathbf{Q}$ denotes the QAM/PSK modulated symbols. Then we can have that $B_t = B*R_C$, where R_C is the SFBC code rate. In order to use the space-frequency gain, the length of each input block of the OFDM system is assumed equal to B. The output of the SFBC encoder is $\mathbf{F}$, and it contains X_T data blocks, $\{\mathbf{F}_1, \mathbf{F}_2, \ldots \mathbf{F}_{X_T}\}$. Then, the transmission matrix after IFFT block, $\mathbf{P}=\{\mathbf{P}_1, \mathbf{P}_2, \ldots, \mathbf{P}_{X_T}\}$, indicating that the signal from the first antenna to the $X_T{}^{th}$ antenna needs to be transmitted. And it can be expressed as, $\mathbf{P}=\mathbf{F}\mathbf{E}^-$, where $\mathbf{E}^-(k, s) = e^{j2\pi(k-1)(s-1)/B}$.

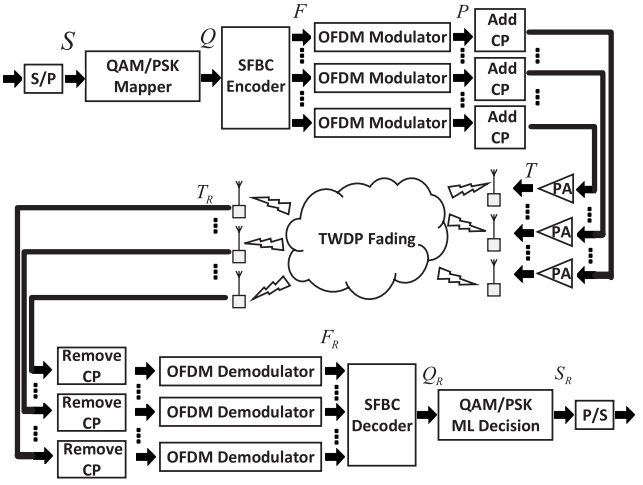

FIGURE 1. The framework of SFBC MIMO-OFDM system with nonlinear power amplifiers; The lengths of IFFT and FFT block are equal.

For simplicity, we define the system operating point as E_P, which denotes the sum of the input power of the X_T antennas into the PA, and it can be written as,

$$E_P = \frac{1}{B}\sum_{t=1}^{X_T}\sum_{b=1}^{B-1} E(\mathbf{P}(t,b) \times \mathbf{P}^*(t,b)) = \frac{X_T}{R_c}\sum_{n=0}^{B_t-1} E(\mathbf{Q}(n,1) \times \mathbf{Q}^*(n,1)) \quad (1)$$

As shown in Fig.1, the signal to be transmitted enters the PA and it can be expressed as the nonlinearly amplified transmission matrix $\mathbf{T}$, where $\mathbf{T} = \alpha_0 \times \mathbf{P} + \mathbf{D}_{non}$ [18], [19]. In this formula, α_0 is the amplification factor of PA and $\mathbf{D}_{non}$ denotes the nonlinear noise that PA produces. The nonlinear distortion of PA leads to the reproduction of the spectrum, and $\mathbf{D}_{non}$ is closely related to the fading of the inter modulation product on the OFDM subcarriers [17].

We assume that the fading process in each OFDM block remains stationary and it varies from one block to another. Different receive antennas are considered irrelevant for the relevant fading process, and we assume full synchronization. Therefore, at the receiver, after removing the cyclic prefix, the received signal $\mathbf{T}_R$ can be written as,

$$\mathbf{T}_R = \mathbf{H}\mathbf{T} + \mathbf{D}_{ch} = \mathbf{H}(\alpha_0\mathbf{P} + \mathbf{D}_{non}) + \mathbf{D}_{ch} \tag{2}$$

where $\mathbf{D}_{ch}$ represents channel noise and its uncorrelated elements follow $Nd(0, \sigma_{ch}^2)$. $\mathbf{H}$ represents the TWDP channel matrix and the element $\mathbf{H}(j, i)$ describes the fading impulse response of the channel between the i^{th} transmit antenna and the j^{th} receive antenna. Furthermore, the fading envelope has TWDP statistics and the instantaneous SNR per symbol has an approximate PDF given in [20] as,

$$p_\gamma(\gamma) = \frac{\hat{K}}{2\bar{\gamma}} \sum_{i=1}^{L} \sum_{j=0}^{1} \exp\left(-P_{2i-j} - \frac{\hat{K}\gamma}{\bar{\gamma}}\right) \times C_i I_0\left(2\sqrt{A_{i,j}}\right) \tag{3}$$

where $\hat{K} = K + 1$, K is the ratio of total specular power to total diffuse power, $P_{2i} = \left(\hat{K} - 1\right)(1 + \alpha_i)$, $P_{2i-1} = \left(\hat{K} - 1\right)(1 - \alpha_i)$, $\alpha_i = \delta \cos\left(\pi(i-1)/2L - 1\right)$, δ is the relative strength of two specular components, C_i is constant coefficient whose length depends on L and the first five exact values are given in [20]. $\bar{\gamma}$ is the average SNR, L is the order of TWDP PDF, $A_{i,j} = P_{2i-j}\hat{K}\gamma/\bar{\gamma}$ and I_0 is the modified Bessel function of first kind and zeroth order.

The exact MGF of TWDP fading will be required in order to derive the closed-form expressions of BER and the exact MGF of TWDP fading has been recently given in [21] as,

$$M_\gamma(s) = \frac{\hat{K}}{\hat{K} - s\bar{\gamma}} \exp\left(\frac{(\hat{K}-1)s\bar{\gamma}}{\hat{K} - s\bar{\gamma}}\right) I_0\left(\frac{(\hat{K}-1)s\bar{\gamma}\Omega}{\hat{K} - s\bar{\gamma}}\right) \tag{4}$$

where Ω denotes the ratio of the peak specular power to the average specular power. Considering that the channel is not perfectly known at the receiver, the received signal can be rewritten as,

$$\begin{aligned}\mathbf{T}_R &= (\hat{\mathbf{H}} + \mathbf{e})\mathbf{T} + \mathbf{D}_{ch} \\ &= (\hat{\mathbf{H}} + \mathbf{e})(\alpha_0\mathbf{P} + \mathbf{D}_{non}) + \mathbf{D}_{ch}\end{aligned} \tag{5}$$

where we assume a minimum mean squared error of channel estimate and define $\hat{\mathbf{H}} = \mathbf{H} - \mathbf{e}$, and $\mathbf{e}$ is the receiver's estimation error.

After OFDM demodulation, the received decoding signal can be expressed as,

$$\begin{aligned}\mathbf{F}_R &= \mathbf{T}_R\mathbf{E}^+ = ((\hat{\mathbf{H}} + \mathbf{e})(\alpha_0\mathbf{P} + \mathbf{D}_{non}) + \mathbf{D}_{ch})\mathbf{E}^+ \\ &= \alpha_0(\hat{\mathbf{H}} + \mathbf{e})\mathbf{P}\mathbf{E}^+ + (\hat{\mathbf{H}} + \mathbf{e})\mathbf{D}_{non}\mathbf{E}^+ + \mathbf{D}_{ch}\mathbf{E}^+\end{aligned} \tag{6}$$

where $\mathbf{E}^+$ is a matrix, express FFT operation on the signal, $\mathbf{E}^+(k, s) = Bs^{-1}e^{-j2\pi(k-1)(s-1)/B}$. Here we define $\mathbf{D}_{rec} = (\hat{\mathbf{H}} + \mathbf{e})\mathbf{D}_{non}\mathbf{E}^+ + \mathbf{D}_{ch}\mathbf{E}^+$, which denotes the noise component at the receiver. As we can see, the noise component contains the nonlinear distortion and the channel noise.

In nonlinear MIMO-OFDM system, $\left[\mathbf{D}_{non}\mathbf{E}^+\right](r, s)$ can be modeled as a Gaussian signal, as indicated by [22] and [23]. Therefore, it can be known that $\left[\mathbf{H}\mathbf{D}_{non}\mathbf{E}^+\right](r, s)$ is also a Gaussian signal and is equivalent to the SISO model, [24], [25]. Furthermore, $\mathbf{D}_{rec}$ follows distribution $Nd(0, \sigma_\eta^2)$ [24],

$$\begin{aligned}\sigma_\eta^2 = \frac{1}{X_R B} \sum_{r=1}^{X_R} \sum_{n=1}^{B} \\ \times \begin{cases} E\left(\left[\mathbf{D}_{ch}\mathbf{E}^+\right](r, n) \times \left[\mathbf{D}_{ch}\mathbf{E}^+\right]^*(r, n)\right) \\ +E\left(\left[(\hat{\mathbf{H}} + \mathbf{e})\mathbf{D}_{non}\mathbf{E}^+\right](r, n) \times \right. \\ \left. \left[(\hat{\mathbf{H}} + \mathbf{e})\mathbf{D}_{non}\mathbf{E}^+\right]^*(r, n)\right) \end{cases}\end{aligned} \tag{7}$$

Considering that $\hat{\mathbf{H}} + \mathbf{e}$ is a normalized $X_R \times X_T$ matrix and $\mathbf{E}^+$ represents an FFT operation, the above equation can be modified to,

$$\begin{aligned}\sigma_\eta^2 &= \frac{1}{B}\sigma_{ch}^2 + \frac{1}{B}\sigma_{non}^2 \\ &= \frac{1}{B}\sigma_{ch}^2 + \frac{1}{B}\sum_{t=1}^{X_T}\sum_{n=1}^{B} E\left(\begin{array}{c}\left[\mathbf{D}_{non}\mathbf{E}^+\right](t, n) \\ \times \left[\mathbf{D}_{non}\mathbf{E}^+\right]^*(t, n)\end{array}\right)\end{aligned} \tag{8}$$

Here, $E\left(\left|\left[\mathbf{D}_{non}\mathbf{E}^+\right](t, n)\right|^2\right)$ denotes the power of the fading term of the n^{th} OFDM subcarrier through the t^{th} transmission path. The total energy of the symbols transmitted by X_T antennas can be normalized to X_T. Therefore, we can express the average SNR at each receiver, i.e., receiver SNR, and it can be written as,

$$\gamma_{rec} = \frac{\alpha_0{}^2 E_P}{B\sigma_\eta^2} = \frac{\alpha_0{}^2 E_P}{\sum_{t=1}^{X_T}\sum_{n=1}^{B} E\left(\left|\left[\mathbf{D}_{non}\mathbf{E}^+\right](t, n)\right|^2\right) + \sigma_{ch}^2} \tag{9}$$

III. CHANNEL CAPACITY OF NONLINEAR SFBC MIMO-OFDM SYSTEM UNDER IMPERFECT CSI

This section derives lower and upper bounds of mutual information for nonlinear SFBC MIMO-OFDM system given an estimated channel knowledge $\hat{\mathbf{H}}$ first. And then we derive the channel capacity under imperfect CSI and the optimal power allocation strategy to achieve it over spatial (antenna) and temporal (fading) domains.

A. LOWER AND UPPER BOUNDS OF MUTUAL INFORMATION

In this subsection, to obtain a lower bound of mutual information $I(\mathbf{T};\mathbf{T}_R|\hat{\mathbf{H}})$ given an estimated channel knowledge $\hat{\mathbf{H}}$, we can expand the mutual information into differential entropies as,

$$I(\mathbf{T};\mathbf{T}_R|\hat{\mathbf{H}})=h(\mathbf{T}|\hat{\mathbf{H}})-h(\mathbf{T}|\mathbf{T}_R,\hat{\mathbf{H}}) \tag{10}$$

Here we define $\mathbf{Z}$ as the autocorrelation matrix of the transmitted signal, and it can be written as $\mathbf{Z}=E(\mathbf{T}\mathbf{T}^*)$. Since the entropy of a random vector reaches its maximum when the entropy of a Gaussian random vector with the same variance, $h(\mathbf{T}|\hat{\mathbf{H}})$ can be rewritten as $E[\log_2(\pi e^1\mathbf{Z})]$. $I(\mathbf{T};\mathbf{T}_R|\hat{\mathbf{H}})$ is upper bounded by the entropy of a Gaussian random variable whose variance is equal to the mean square error of the linear MMSE estimate of $\mathbf{T}$ given $\mathbf{T_R}$ and $\hat{\mathbf{H}}$. Therefore, the lower bound of $I(\mathbf{T};\mathbf{T}_R|\hat{\mathbf{H}})$ can be written as,

$$I_{lower}(\mathbf{T};\mathbf{T}_R|\hat{\mathbf{H}}) = E\left(\log_2\left\{\det\left[\boldsymbol{I}_{BX_R}+\frac{\hat{\mathbf{H}}^\dagger\hat{\mathbf{H}}\mathbf{Z}}{\mathbf{I}_{BX_R}\left(\sigma_{ch}^2+\sigma_{non}^2\right)+\sum\mathbf{e}\mathbf{T}}\right]\right\}\right) \tag{11}$$

Considering that the entries of $\mathbf{H}$ are independent and identically distributed, we have that $\sum\mathbf{e}\mathbf{T}=\sigma_{\mathbf{e}}^2P\mathbf{I}_{BX_R}$, where P is the total power of the transmitter and $\sigma_{\mathbf{e}}^2$ dictates the quality of the channel estimation, $\sigma_{\mathbf{e}}^2=E(\mathbf{H}_{ij}^2)-E(\hat{\mathbf{H}}_{ij}^2)$. Therefore, $I_{lower}(\mathbf{T};\mathbf{T}_R|\hat{\mathbf{H}})$ can be rewritten as,

$$I_{lower}(\mathbf{T};\mathbf{T}_R|\hat{\mathbf{H}}) = E\left(\log_2\left\{\det\left[\mathbf{I}_{BX_R}+\frac{\hat{\mathbf{H}}^\dagger\hat{\mathbf{H}}\mathbf{Z}}{\mathbf{I}_{BX_R}\left(\left(\sigma_{ch}^2+\sigma_{non}^2\right)+\sigma_{\mathbf{e}}^2P\right)}\right]\right\}\right) \tag{12}$$

On the other hand, we expand the mutual information in an alternate way to obtain an upper bound,

$$I(\mathbf{T};\mathbf{T}_R|\hat{\mathbf{H}})=h(\mathbf{T}_R|\hat{\mathbf{H}})-h(\mathbf{T}_R|\mathbf{T},\hat{\mathbf{H}}) \tag{13}$$

Similar to the maximum value of $h(\mathbf{T}|\hat{\mathbf{H}})$, using the fact that the Gaussian distribution maximizes the entropy over all distributions with the same covariance and we can get that,

$$h(\mathbf{T}_R|\hat{\mathbf{H}})\le E\left[\log_2\det\left(\pi e^1\left(\frac{\hat{\mathbf{H}}\mathbf{Z}\hat{\mathbf{H}}^\dagger+\sigma_{\mathbf{e}}^2P\mathbf{I}_{BX_R}}{\left(\sigma_{ch}^2+\sigma_{non}^2\right)\mathbf{I}_{BX_R}}\right)\right)\right] \tag{14}$$

Here we define $\mathbf{e}$ as complex Gaussian, and $(\mathbf{T}_R|\mathbf{T},\hat{\mathbf{H}})$ is complex Gaussian with $Nd(\hat{\mathbf{H}}\mathbf{T},\sum\mathbf{e}\mathbf{T}+\mathbf{I}_{BX_R})$. Therefore, $h(\mathbf{T}_R|\mathbf{T},\hat{\mathbf{H}})$ can be written as,

$$h(\mathbf{T}_R|\mathbf{T},\hat{\mathbf{H}})=E_{\mathbf{T}}\left[\log_2\det\left(\frac{\pi e^1\mathbf{I}_{BX_R}+\sigma_{\mathbf{e}}^2||\mathbf{T}||^2\mathbf{I}_{BX_R}}{+\left(\sigma_{ch}^2+\sigma_{non}^2\right)\mathbf{I}_{BX_R}}\right)\right] \tag{15}$$

Then, the upper bound of the mutual information can be expression as,

$$I_{upper}(\mathbf{T};\mathbf{T}_R|\hat{\mathbf{H}}) = I_{lower}(\mathbf{T};\mathbf{T}_R|\hat{\mathbf{H}})+\mathbf{X}_RE_{\mathbf{T}}\left[\log_2\frac{\sigma_{\mathbf{e}}^2P+1}{\sigma_{\mathbf{e}}^2||\mathbf{T}||^2+1}\right] \tag{16}$$

B. CHANNEL CAPACITY AND OPTIMAL POWER ALLOCATION

The ergodic capacity of nonlinear SFBC MIMO-OFDM system, with an estimated $\hat{\mathbf{H}}$ known at the transmitter and the receiver, is given by [26] and it can be expressed as,

$$C=\max_{p(\mathbf{T}|\hat{\mathbf{H}})}I(\mathbf{T};\mathbf{T}_R|\hat{\mathbf{H}}) \tag{17}$$

where $p(\mathbf{T}|\hat{\mathbf{H}})$ is the probability distribution of $\mathbf{T}$ given $\hat{\mathbf{H}}$. In this subsection, to obtain a lower bound of channel capacity, we need to find the optimal input covariance matrix $\mathbf{Z}$ that maximizes $I_{lower}(\mathbf{T};\mathbf{T}_R|\hat{\mathbf{H}})$. Let the singular value decomposition of the estimated channel matrix be $\hat{\mathbf{H}}=\mathbf{U}\mathbf{D}\mathbf{V}^*$, where $\mathbf{U}$ and $\mathbf{V}$ are unitary and $\mathbf{D}$ is diagonal, and let us define two quantities, $\tilde{\mathbf{Z}}=\mathbf{V}^*\mathbf{Z}\mathbf{V}$ and $\mathbf{K}=\mathbf{D}^*\mathbf{D}$. Then $I_{lower}(\mathbf{T};\mathbf{T}_R|\hat{\mathbf{H}})$ can be written as,

$$I_{lower}(\mathbf{T};\mathbf{T}_R|\hat{\mathbf{H}}) = \log_2\left\{\det\left[\mathbf{I}_{BX_R}+\frac{\mathbf{K}\tilde{\mathbf{Z}}}{\left(\sigma_{ch}^2+\sigma_{non}^2\right)+P\sigma_e^2}\right]\right\} \tag{18}$$

Under an average power constraint $E(P)=E(trace(\mathbf{Z}))\le{\alpha_0}^2E_P$, observing that $trace(\mathbf{Z})=trace(\tilde{\mathbf{Z}})$, $I_{lower}(\mathbf{T};\mathbf{T}_R|\hat{\mathbf{H}})$ is maximized with $\tilde{\mathbf{Z}}$ a diagonal matrix, $\tilde{\mathbf{Z}}=diag(P_1,\ldots,P_{X_T})$, with an optimal power distribution $\{P_i\}$ such that $\sum_{i=1}^{X_T}P_i={\alpha_0}^2E_P$. Thus, the lower bound of ergodic capacity is given by,

$$C_{lower}=\max_{\{P_i\}}E\left(\sum_{i=1}^{X_T}log_2\left(\frac{\left(\sigma_{ch}^2+\sigma_{non}^2\right)+P\sigma_{\mathbf{e}}^2+P_i\lambda_i}{\left(\sigma_{ch}^2+\sigma_{non}^2\right)+P\sigma_{\mathbf{e}}^2}\right)\right)$$
$$subject\ to\ E(P)=E(\sum_{i=1}^{X_T}P_i)\le{\alpha_0}^2E_P \tag{19}$$

where λ_i is the $(i,i)^{th}$ element of $\mathbf{K}$ and thus the i^{th} eigenvalue of $\hat{\mathbf{H}}^*\hat{\mathbf{H}}$. The above expectations are performed over the joint distribution of $(\lambda_1,\ldots,\lambda_{X_T})$. The input to the channel that achieves the capacity has covariance matrix of the form $\mathbf{Z}=\mathbf{V}diag(P_1,\ldots,P_{X_T})\mathbf{V}^*$ whose optimal subchannel powers $\{P_i\}$ are determined as functions of $(\lambda_1,\ldots,\lambda_{X_T})$.

As we have seen, C_{lower} is the supremum of achievable data rates in practical transmission systems that employ Gaussian codebooks and nearest neighbor decoders. Moreover, we have seen that the difference between C_{lower} and the exact capacity is small for Gaussian inputs unless $X_R\gg X_T$. Hence, we treat C_{lower} as a performance measure and concentrate on deriving the optimal power allocation strategy to achieve it.

In TWDP fading channels, the optimal $\mathbf{Z}$ that maximizes C_{lower} is spatially white, i.e., $\mathbf{Z}=(P/X_T)\mathbf{I}_{BX_R}$. Moreover, it can be verified by using Jensen's inequality that the temporal power adaptation does not increase the capacity, i.e., $P={\alpha_0}^2E_P$. Therefore, the capacity lower bound is given by,

$$C_{lower}=E\left(\sum_{i=1}^{X_T}log_2\left(1+\frac{{\alpha_0}^2E_P/X_T}{\left(\sigma_{ch}^2+\sigma_{non}^2\right)+{\alpha_0}^2E_P\sigma_{\mathbf{e}}^2}\lambda_i\right)\right) \tag{20}$$

Therefore, we can show that the lower bound of channel capacity can be expressed as,

$$\begin{aligned} C &= E\left(\log_2\left\{\det\left[I_{BX_R}+\frac{\hat{H}\hat{H}^{\dagger}}{X_T}\times\frac{{\alpha_0}^2E_P}{(\sigma_{ch}^2+\sigma_{non}^2)+{\alpha_0}^2E_P\sigma_e^2}\right]\right\}\right) \\ &= E\left(\log_2\left\{\det\left[I_{BX_R}+\frac{\hat{H}\hat{H}^{\dagger}}{X_T}\times\frac{\gamma_{rec}}{1+\gamma_{rec}\sigma_e^2}\right]\right\}\right) \\ &= E\left(\log_2\left\{\det\left[I_{BX_R}+\frac{\hat{H}\hat{H}^{\dagger}}{X_T}\times\gamma_{ce}\right]\right\}\right) \end{aligned} \tag{21}$$

where γ_{ce} denotes the SNR at the receiver under imperfect CSI.

IV. BER ANALYSIS OF NONLINEAR SFBC MIMO-OFDM SYSTEM UNDER IMPERFECT CSI

This section derives the average BER of nonlinear SFBC OFDM system under imperfect CSI for both QAM and PSK signals. The closed-form expression of average BER can be obtained by averaging the conditional BER for AWGN channels over the PDF of the output SNR γ. Mathematically, the average BER $\overline{\mu}_{MQAM/MPSK}$ can be determined as,

$$\overline{\mu}_{MQAM/MPSK}=\int_0^{\infty}\mu_{MQAM/MPSK}\times p(\gamma)d\gamma \tag{22}$$

where, $p(\gamma)$ is the PDF of γ and $\mu_{MQAM/MPSK}$ is the conditional BER of the modulation scheme in AWGN channel.

A. NONLINEAR MQAM-SFBC-OFDM WITH IMPERFECT CSI

In this subsection, the closed-form expressions of BER for MQAM nonlinear SFBC OFDM system under imperfect CSI over TWDP fading channel are derived.

At the receiver of the SFBC OFDM system, the decoder outputs the decoded signal by minimizing the decision matrix, $|\widetilde{q}[k]-q[k]|^2, k=0,\ldots,B-1$. And the decoded signal can be written as,

$$\mathbf{Q}_R=\frac{1}{R_C}\alpha_0||\hat{\mathbf{H}}||_F^2\mathbf{Q}+\mathbf{W} \tag{23}$$

where Q and Q_R represents the source PSK/QAM symbols and post decoding symbols, respectively; $\mathbf{W}$ represents the noise part and follows distribution $Nd(0,\frac{1}{R_C}||\hat{\mathbf{H}}||_F^2\sigma_\eta^2)$ [24],

Therefore, we can express the normalized instantaneous SNR after the SFBC decoding as [13],

$$\gamma_{dec}=\frac{1}{X_TR_C}\sum_{j=1}^{X_R}\sum_{i=1}^{X_T}|\mathbf{H}(j,i)|^2\gamma_{ce} \tag{24}$$

Then, using the expression for the SNR in eq.(21), γ_{ce} can be written as,

$$\begin{aligned}\gamma_{ce}&=\frac{\gamma_{rec}}{1+\gamma_{rec}\sigma_{\mathbf{e}}^2} \\ &=\frac{{\alpha_0}^2E_P}{\left(\sum_{t=1}^{X_T}\sum_{n=1}^{B}E\left(\left|\left[\mathbf{D}_{non}\mathbf{E}^{+}\right](t,n)\right|^2\right)+\sigma_{ch}^2+{\alpha_0}^2E_P\sigma_{\mathbf{e}}^2\right)}\end{aligned} \tag{25}$$

Then, apply eq.(25) into eq.(24), the instantaneous SNR for SFBC OFDM over TWDP fading channels under imperfect CSI after the SFBC decoding can be rewritten as,

$$\gamma_{dec}=\frac{{\alpha_0}^2E_P\times\sum_{j=1}^{X_R}\sum_{i=1}^{X_T}|\mathbf{H}(j,i)|^2}{X_TR_C\left(\sum_{t=1}^{X_T}\sum_{n=1}^{B}E\left(\left|\left[\mathbf{D}_{non}\mathbf{E}^{+}\right](t,n)\right|^2\right)+\sigma_{ch}^2+{\alpha_0}^2E_P\sigma_{\mathbf{e}}^2\right)} \tag{26}$$

In [23] and [22], $E\left(\left|\left[\mathbf{D}_{non}\mathbf{E}^{+}\right](t,n)\right|^2\right)$ is derived from the spectral analysis of nonlinear distortion, and its complex expression makes it difficult to bring it to the extended analysis of SNR behavior. In [27], a new expression is derived through the analysis of the inter-modulation product,

$$E\left(\left|\left[\mathbf{D}_{non}\mathbf{E}^{+}\right](t,n)\right|^2\right)=\sum_{\substack{\sum d_m=1,\sum|d_m|=\theta\geq3,\\ \sum m\times d_m=n,\max(|d_m|)=1}}\left|\sum_{g=1}^{G}\left[h_g\times\prod_{m=1}^{B}J_{d_m}\left(\frac{2g\pi}{D_{\text{mod}}}\sqrt{\frac{E_P}{X_TB}}\right)\right]\right|^2 \tag{27}$$

where d_m can be any integer, and J_{d_m} represents the first term of the d_m^{th} order Bessel equation. D_{mod} and h_g represent the dynamic range of models and the coefficients of the G order Bessel-Fourier PA model, respectively.

Considering that $J_{-1}(z)=-J_1(z)$, the equation can be rewritten as,

$$E\left(\left|\left[\mathbf{D}_{non}\mathbf{E}^{+}\right](t,n)\right|^2\right)=\sum_{\kappa=3,5,\ldots}\lambda(\kappa,E_P)\times\rho(\kappa,n) \tag{28}$$

where $\rho(\kappa,n)$ denotes the number of κ^{th} order inter-modulation product in the n^{th} OFDM subcarrier, and it dose not depend on the characteristics of PA and the total power E_P. For example, for the 64-point FFT OFDM signal in this paper, $\sum_{b=1}^{B}\rho(\kappa,3)=82000$. At the same time, the feature vector of IMP satisfies condition: $\sum d_m=1,\sum d_m\times m=n,\sum|d_m|=\theta\geq3,\max(|d_m|)=1$.

What's more, the average power of individual IMPs, i.e., $\lambda(\kappa,E_P)$ can be obtained by an unique IMP analysis [27], i.e.,

$$\lambda(\kappa,E_P)=\left|\sum_{g=1}^{G}\left[h_g\times J_{d_m}^{\kappa}\left(\frac{2g\pi}{D_{\text{mod}}}\sqrt{\frac{E_P}{X_TB}}\right)\times J_0^{B-\kappa}\left(\frac{2g\pi}{D_{\text{mod}}}\sqrt{\frac{E_P}{X_TB}}\right)\right]\right|^2 \tag{29}$$

Apply eq.(28) into eq.(26), γ_{dec} can be rewritten as,

$$\gamma_{dec} = \frac{B \times \lambda(1, E_P) \sum_{j=1}^{X_R} \sum_{i=1}^{X_T} |\mathbf{H}(j,i)|^2}{R_C \left(X_T \sum_{\kappa=3,5,\ldots} \left[\lambda(\kappa, E_P) \times \left(\sum_{n=1}^{B} \rho(\kappa, n) \right) \right] + \sigma_{ch}^2 + \sigma_{\mathbf{e}}^2 \left(X_T B \times \lambda(1, E_P) \right) \right)} \tag{30}$$

Considering that the third order IMPs dominate the nonlinear distortion, eq.(30) can be rewritten as,

$$\gamma_{dec} = \frac{B \times \lambda(1, E_P) \sum_{j=1}^{X_R} \sum_{i=1}^{X_T} |\mathbf{H}(j,i)|^2}{R_C \left(X_T \lambda(3, E_P) \times \left(\sum_{n=1}^{B} \rho(3, n) \right) + \sigma_{ch}^2 + \sigma_{\mathbf{e}}^2 \left(X_T B \times \lambda(1, E_P) \right) \right)} \tag{31}$$

As shown in Fig. 1, the output of SFBC decoder, i.e., Q_R, is driven to QAM/PSK ML Decision block and is demodulated to the bit stream. We assume that the system uses a square MQAM modulation scheme of Gray code, and the symbol rate for sub-channel is $\rho = (\log_2 M) bit/symbol$. Then, the BER of the b^{th} sub-channel, μ_{b-MQAM} can be expressed as [28],

$$\mu_{b-MQAM} = \frac{2\sqrt{2^\rho} - 2}{\rho\sqrt{2^\rho}} erfc\left(\sqrt{\frac{1.5\xi\alpha_0{}^2 E_P}{(2^\rho - 1)(\sigma_{ch}^2 + \sigma_{non}^2 + \sigma_{\mathbf{e}}^2 \alpha_0{}^2 E_P)}} \right) \tag{32}$$

where we define a variable ξ and it can be written as,

$$\xi = \frac{\sum_{j=1}^{X_R} \sum_{i=1}^{X_T} |\mathbf{H}_b(j,i)|^2}{X_T R_C} \tag{33}$$

A tight bound of eq.(32) is given by [29] and can be expressed as,

$$\mu_{b-MQAM} = 0.2 \exp\left(-\frac{1.6\xi\alpha_0{}^2 E_P}{(M-1)(\sigma_{ch}^2 + \sigma_{non}^2 + \sigma_e^2 \alpha_0{}^2 E_P)} \right) \tag{34}$$

Now, the BER of nonlinear MQAM SFBC-OFDM system under imperfect CSI can be expressed as,

$$\mu_{b-MQAM} = \frac{0.2}{B} \times \sum_{b=0}^{B-1} \exp\left(-\frac{1.6\xi\alpha_0{}^2 E_P}{(M-1)(\sigma_{ch}^2 + \sigma_{non}^2 + \sigma_e^2 \alpha_0{}^2 E_P)} \right) \tag{35}$$

The average BER (ABER) for nonlinear MQAM SFBC OFDM under imperfect CSI system can now be derived by substituting eq.(35) in eq.(22) as,

$$\begin{aligned} \overline{\mu}_{MQAM} &= \int_0^\infty \cdots \int_0^\infty \mu_{b-MQAM} p(\gamma_{1,1}) \ldots p(\gamma_{X_R,X_T}) \, d\gamma_{1,1} \ldots d\gamma_{X_R,X_T} \\ &= \int_0^\infty \cdots \int_0^\infty \frac{0.2}{B} \sum_{b=0}^{B-1} \exp\left(-\frac{1.6\xi\alpha_0{}^2 E_P}{(M-1)(\sigma_{ch}^2 + \sigma_{non}^2 + \sigma_{\mathbf{e}}^2 \alpha_0{}^2 E_P)} \right) \\ &\quad p(\gamma_{1,1}) \ldots p(\gamma_{X_R,X_T}) d\gamma_{1,1} \ldots d\gamma_{X_R,X_T} \end{aligned} \tag{36}$$

where we define $\gamma_{j,i} = \gamma_{ce} |\mathbf{H}_b(j,i)|^2$, and $p(\gamma_{j,i})$ is the PDF of $\gamma_{j,i}$ as defined in eq.(3). Then the above expression can be further simplified into,

$$\begin{aligned} \overline{\mu}_{MQAM} &= \frac{0.2}{B} \sum_{b=0}^{B-1} \int_0^\infty f(\gamma_{1,1}) p(\gamma_{1,1}) d\gamma_{1,1} \\ &\quad \ldots \int_0^\infty f(\gamma_{X_R,X_T}) p(\gamma_{X_R,X_T}) d\gamma_{X_R,X_T} \end{aligned} \tag{37}$$

where $f(\gamma_{i,j}) = \exp\left(\frac{-1.6\gamma_{i,j}}{(M-1)X_T R_C} \right)$. The above equation can be easily solved using MGF approach because,

$$M_{\gamma_{i,j}}(-1.6/((M-1)X_T R_C)) = \int_0^\infty f(\gamma_{i,j}) p(\gamma_{i,j}) d\gamma_{i,j} \tag{38}$$

Finally, substituting eq.(4) and eq.(31) into eq.(37), we can express the closed-form expression of ABER for nonlinear SFBC OFDM system using MQAM modulation under imperfect CSI as,

$$\overline{\mu}_{MQAM} = 0.2 \left(\frac{\Phi\hat{K}}{\Phi\hat{K} - 1.6\alpha_0{}^2 E_P} \exp\left(\frac{1.6\alpha_0{}^2 E_P(\hat{K}-1)}{\Phi\hat{K} - 1.6\alpha_0{}^2 E_P} \right) \times I_0\left(\frac{1.6\alpha_0{}^2 E_P(\hat{K}-1)\Omega}{\Phi\hat{K} - 1.6\alpha_0{}^2 E_P} \right) \right)^{X_R X_T} \tag{39}$$

where we define a variable Φ and it can be written as,

$$\begin{aligned} \Phi &= (M-1)X_T R_C \times (\sigma_{ch}^2 + \sigma_{non}^2 + \sigma_{\mathbf{e}}^2 \alpha_0{}^2 E_P) \\ &= (M-1)X_T R_C \times \left(X_T \lambda(3, E_P) \times \left(\sum_{n=1}^{B} \rho(3,n) \right) + \sigma_{ch}^2 + \sigma_{\mathbf{e}}^2 \left(X_T B \times \lambda(1, E_P) \right) \right) \end{aligned} \tag{40}$$

B. NONLINEAR MPSK-SFBC-OFDM WITH IMPERFECT CSI

Using the same approach as for the MQAM case, we can express the BER μ_{b-MPSK} as,

$$\begin{aligned} \mu_{b-MPSK} &= \frac{1}{\rho} erfc\left(\sin\left(\frac{\pi}{M}\right) \times \sqrt{\gamma_{dec}} \right) \\ &= \frac{1}{\rho} erfc\left(\sin\left(\frac{\pi}{M}\right) \times \sqrt{\frac{\xi\alpha_0{}^2 E_P}{(\sigma_{ch}^2 + \sigma_{non}^2 + \sigma_{\mathbf{e}}^2 \alpha_0{}^2 E_P)}} \right) \end{aligned} \tag{41}$$

which can be approximated as [29],

$$\mu_{b-MPSK} = 0.2\exp\left(-\frac{7\xi{\alpha_0}^2 E_P}{(2^{1.9\rho}+1)(\sigma_{ch}^2+\sigma_{non}^2+\sigma_{\hat{\mathbf{e}}}^2{\alpha_0}^2E_P)}\right) \tag{42}$$

Therefore, the BER of nonlinear MPSK SFBC-OFDM system under imperfect CSI can be expressed as,

$$\mu_{b-MPSK} = \frac{0.2}{B}\sum_{b=0}^{B-1}\exp\left(\frac{-7\alpha_0^2E_P\zeta}{(2^{1.9\rho}+1)(\sigma_{ch}^2+\sigma_{non}^2+\sigma_{\hat{\mathbf{e}}}^2\alpha_0^2E_P)}\right) \tag{43}$$

Similar to the derivation of $\overline{\mu}_{MQAM}$, we can get an average expression of $\overline{\mu}_{MPSK}$ by substituting eq.(43) in eq.(22) as,

$$\begin{aligned}\overline{\mu}_{MPSK} &= \int_0^\infty\cdots\int_0^\infty \mu_{b-MPSK}p(\gamma_{1,1})\ldots p(\gamma_{X_R,X_T}) \\ &\quad d\gamma_{1,1}\ldots d\gamma_{X_R,X_T} \\ &= \int_0^\infty\cdots\int_0^\infty \frac{0.2}{B}\sum_{b=0}^{B-1}\exp\left(\frac{-7\xi\alpha_0^2E_P}{(2^{1.9\rho}+1)(\sigma_{ch}^2+\sigma_{non}^2+\sigma_{\hat{\mathbf{e}}}^2\alpha_0^2E_P)}\right) \\ &\quad p(\gamma_{1,1})\ldots p(\gamma_{X_R,X_T})d\gamma_{1,1}\ldots d\gamma_{X_R,X_T}\end{aligned} \tag{44}$$

Finally, substituting eq.(4) and eq.(31) into eq.(44), we can easily show that the ABER is given by,

$$\overline{\mu}_{MPSK} = 0.2\left(\begin{array}{c}\frac{\theta\hat{K}}{\theta\hat{K}-7\alpha_0^2E_P}\exp\left(\frac{7\alpha_0^2E_P(\hat{K}-1)}{\theta\hat{K}-7\alpha_0^2E_P}\right) \\ \times I_0\left(\frac{7\alpha_0^2E_P(\hat{K}-1)\Omega}{\theta\hat{K}-7\alpha_0^2E_P}\right)\end{array}\right)^{X_RX_T} \tag{45}$$

where we define a variable θ and it can be written as,

$$\begin{aligned}\theta &= (X_TR_C2^{1.9\rho}+1)\times(\sigma_{ch}^2+\sigma_{non}^2+\sigma_{\hat{\mathbf{e}}}^2{\alpha_0}^2E_P) \\ &= (X_TR_C2^{1.9\rho}+1)\times\left(X_T\lambda(3,E_P)\times\left(\sum_{n=1}^{B}\rho(3,n)\right)\right. \\ &\quad \left.+\sigma_{ch}^2+\sigma_{\hat{\mathbf{e}}}^2\,(X_TB\times\lambda(1,E_P))\right)\end{aligned} \tag{46}$$

V. ANALYSIS OF OPTIMAL SYSTEM OPERATING POINT

In this section, we will discuss the characteristics of γ_{dec} and analyze the system operating point. When the PA operates in its linear region, the nonlinear distortion is negligible, so we can get $\lambda(3,E_P)\approx 0$. Based on the eq.(31), we can get that,

$$\gamma_{dec}^{Lin} = \lim_{E_P\to 0}\gamma_{dec} = \frac{X_TB\times\lambda(1,E_P)\xi}{\sigma_{ch}^2+\sigma_{\hat{\mathbf{e}}}^2X_TB\lambda(1,E_P)} \tag{47}$$

where γ_{dec}^{Lin} is the behavior of γ_{dec} when a low power E_P applied. Introducing eq.(29) into eq.(47), we can get that,

$$\gamma_{dec}^{Lin} = \frac{\xi E_P\left|\sum_{g=1}^{G}(h_p\frac{p\pi}{D\ \mathrm{mod}})\right|^2}{\sigma_{ch}^2+\sigma_{\hat{\mathbf{e}}}^2E_P\left|\sum_{g=1}^{G}(h_p\frac{p\pi}{D\ \mathrm{mod}})\right|^2} \tag{48}$$

In this equation, we can clearly see that when the PA works in its linear region, the instantaneous SNR γ_{dec} only relates to the symbol energy E_P, the channel estimate error $\sigma_{\hat{\mathbf{e}}}^2$ and the channel noise σ_{ch}^2. Therefore, the performance of γ_{dec}^{Lin} can be obtained as the follows,

$$\frac{\partial\gamma_{dec}^{Lin}}{\partial E_P} = \frac{\xi\sigma_{ch}^2\left|\sum_{g=1}^{G}(h_p\frac{p\pi}{D\ \mathrm{mod}})\right|^2}{\left(\sigma_{ch}^2+\sigma_{\hat{\mathbf{e}}}^2E_P\left|\sum_{g=1}^{G}(h_p\frac{p\pi}{D\ \mathrm{mod}})\right|^2\right)^2} > 0 \tag{49}$$

and,

$$\frac{\partial\gamma_{dec}^{Lin}}{\partial\sigma_{ch}^2} = \frac{-\xi E_P\left|\sum_{g=1}^{G}(h_p\frac{p\pi}{D\ \mathrm{mod}})\right|^2}{\left(\sigma_{ch}^2+\sigma_{\hat{\mathbf{e}}}^2E_P\left|\sum_{g=1}^{G}(h_p\frac{p\pi}{D\ \mathrm{mod}})\right|^2\right)^2} < 0 \tag{50}$$

and,

$$\frac{\partial\gamma_{dec}^{Lin}}{\partial\sigma_{\hat{\mathbf{e}}}^2} = -\xi\left(\frac{E_P\left|\sum_{g=1}^{G}(h_p\frac{p\pi}{D\ \mathrm{mod}})\right|^2}{\sigma_{ch}^2+\sigma_{\hat{\mathbf{e}}}^2E_P\left|\sum_{g=1}^{G}(h_p\frac{p\pi}{D\ \mathrm{mod}})\right|^2}\right)^2 < 0 \tag{51}$$

When the PA operates in nonlinear state, the nonlinear distortion determines the loss of the system, i.e., $\sigma_\eta^2 >> \sigma_{ch}^2$. Therefore, we can have that,

$$\begin{aligned}\gamma_{dec}^{Nlin} &= \lim_{E_P\to\infty}\gamma_{dec} \\ &= \frac{B\times\lambda(1,E_P)\xi}{\lambda(3,E_P)\times\left(\sum_{n=1}^{B}\rho(3,n)\right)+\sigma_{\hat{\mathbf{e}}}^2\,(B\times\lambda(1,E_P))}\end{aligned} \tag{52}$$

The behavior of γ_{dec}^{Nlin} can be found in [23]. What's more, γ_{dec}^{Nlin} is the gradual progression when the input power E_P is high, and it's also the average SNR of the output elements of the OFDM subcarriers output on each PA. Therefore, the performance of γ_{dec}^{Nlin} can be obtained as the follows,

$$\frac{\partial\gamma_{dec}^{Nlin}}{\partial E_P} = \frac{-2\xi E_P\frac{\left(\sum_{n=1}^{B}\rho(3,n)\right)\left|\sum_{g=1}^{G}(h_p\frac{p\pi}{D\ \mathrm{mod}})^3\right|^2}{X_T^2B^3\left|\sum_{g=1}^{G}(h_p\frac{p\pi}{D\ \mathrm{mod}})\right|^2}}{\left(\sigma_{\hat{\mathbf{e}}}^2+\frac{E_P^2\left(\sum_{n=1}^{B}\rho(3,n)\right)\left|\sum_{g=1}^{G}(h_p\frac{p\pi}{D\ \mathrm{mod}})^3\right|^2}{X_T^2B^3\left|\sum_{g=1}^{G}(h_p\frac{p\pi}{D\ \mathrm{mod}})\right|^2}\right)^2} < 0 \tag{53}$$

and,

$$\frac{\partial \gamma_{dec}^{Nlin}}{\partial \sigma_{\mathbf{e}}^2} = \frac{-\xi}{\left(\sigma_{\mathbf{e}}^2 + \frac{E_P^2\left(\sum_{n=1}^{B}\rho(3,n)\right)\left|\sum_{g=1}^{G}(h_p\frac{p\pi}{D\ \mathrm{mod}})^3\right|^2}{X_T^2B^3\left|\sum_{g=1}^{G}(h_p\frac{p\pi}{D\ \mathrm{mod}})\right|^2}\right)^2} < 0 \tag{54}$$

and $\frac{\partial \gamma_{dec}^{Nlin}}{\partial \sigma_{ch}^2} = 0$.

It can be clearly seen that γ_{dec}^{Lin} and γ_{dec}^{Nlin} follow monotonically increasing or decreasing, as denoted by eq.(49) and eq.(53). Therefore, the maximum value of γ_{dec}, written as $\gamma_{dec-\max}$, will exist. And it shows that the damage of the system is transformed from being initially affected by channel noise to dominated by nonlinear distortion. We define E_{P-best} as the optimal operating point of the SFBC MIMO OFDM system corresponding to $\gamma_{dec-\max}$. Since the channel noise power level is much lower than the PA output power, when E_P has its corresponding E_{P-best}, the work area of PA far exceeds its linear area. Then we can have that,

$$\gamma_{dec-\max} = \frac{\xi X_T B \times \lambda(1, E_{P-best})}{\left(X_T\lambda(3, E_{P-best}) \times (\sum_{n=1}^{B}\rho(3,n)) + \sigma_{ch}^2 + \sigma_{\mathbf{e}}^2 X_T B \times \lambda(1, E_{P-best})\right)} \tag{55}$$

Applied with eq.(29), eq.(55) can be rewritten as,

$$\gamma_{dec-\max} = \frac{\xi X_T^2B^3E_{P-best}\left|\sum_{g=1}^{G}(\frac{h_gp\pi}{D\ \mathrm{mod}})\right|^2}{\left(\sigma_{\mathbf{e}}^2X_T^2B^3E_{P-best}\left|\sum_{g=1}^{G}(\frac{h_gp\pi}{D\ \mathrm{mod}})\right|^2 + X_T^2B^3\sigma_{ch}^2 + (E_{P-best})^3\left|\sum_{g=1}^{G}h_g\left(\frac{p\pi}{D\ \mathrm{mod}}\right)^3\right|^2\left(\sum_{n=1}^{B}\rho(3,n)\right)\right)} \tag{56}$$

Considering that when γ_{dec} is at its maximum, its derivative for E_P is 0. And E_P has its optimal value E_{P-best}. Therefore, we can get that,

$$\begin{aligned}\frac{d\gamma_{dec}}{dE_P} &= 0\\ \Leftrightarrow\ & 2(E_{P-best})^3\left|\sum_{p=1}^{P}h_g(\frac{p\pi}{D\ \mathrm{mod}})^3\right|^2\left(\sum_{n=1}^{B}\rho(3,n)\right)\\ &= X_T^2B^3\sigma_{ch}^2\end{aligned} \tag{57}$$

Then, it can be obtained from eq.(57) that,

$$E_{P-best} = \sqrt[3]{\frac{X_T^2B^3\sigma_{ch}^2}{2\left|\sum_{p=1}^{P}h_g\left(\frac{p\pi}{D\ \mathrm{mod}}\right)^3\right|^2 \times \left(\sum_{n=1}^{B}\rho(3,n)\right)^2}} \tag{58}$$

Here, eq.(58) shows an analytic expression of E_{P-best}, which is related to $\gamma_{dec-\max}$. Bring eq.(58) into eq.(56), we can have that (59), shown at the bottom of this page.

VI. SIMULATION AND DISCUSSION

In this section, the results of the analysis of BER and E_{P-best} derived in Section IV are verified in simulations using various system configurations, and the analysis of the channel capacity derived in Section III is also verified. In addition, TD performance was also studied. The over-sampling rate of OFDM symbols is 4 and B is 64 with cyclic prefix $B/4$. The length of OFDM block is also set as 64. The example PA is measured from an S-band LDMOS solid state PA (SSPA) and its finite variation in AM/PM conversion over the operating range is ignored. Here, the input and output amplitudes of the example LDMOS PA are normalized with respect to the input and output amplitudes of their 1 dB compression point (P1 dB). The tested modulation schemes in simulation include QPSK, 16QAM, and 64QAM.

The analytical and simulated BER using different modulation schemes are plotted in Fig.2. As shown in the derivation, the QPSK signal has better BER performance than the 16QAM and 64QAM signals. The E_{P-best}, which corresponding to the BER lower bound, is independent of the modulation schemes as shown in eq.(58). In order to demonstrate the proximity between the analysis and the simulation results, we define the absolute relative difference percentage, which is the same in [14]. The calculation results of absolute relative difference percentage shows that the average percentage of QPSK is 6.3742%, while the average percentages of 16QAM and 64QAM are 23.5328% and 13.5443%, respectively. It can

$$\gamma_{dec-\max} = \xi\left(\frac{X_T^2B^3\sigma_{ch}^2\left|\sum_{g=1}^{G}(\frac{h_gp\pi}{D\ \mathrm{mod}})\right|^6}{2\left|\sum_{p=1}^{P}h_g\left(\frac{p\pi}{D\ \mathrm{mod}}\right)^3\right|^2 \times \left(\sum_{n=1}^{B}\rho(3,n)\right)^2}\right)^{\frac{1}{3}} \times \left(\sigma_{\boldsymbol{e}}^2\left(\frac{X_T^2B^3\sigma_{ch}^2\left|\sum_{g=1}^{G}(\frac{h_gp\pi}{D\ \mathrm{mod}})\right|^6}{2\left|\sum_{p=1}^{P}h_g\left(\frac{p\pi}{D\ \mathrm{mod}}\right)^3\right|^2 \times \left(\sum_{n=1}^{B}\rho(3,n)\right)^2}\right)^{\frac{1}{3}} + \frac{3}{2}\sigma_{ch}^2\right)^{-1} \tag{59}$$

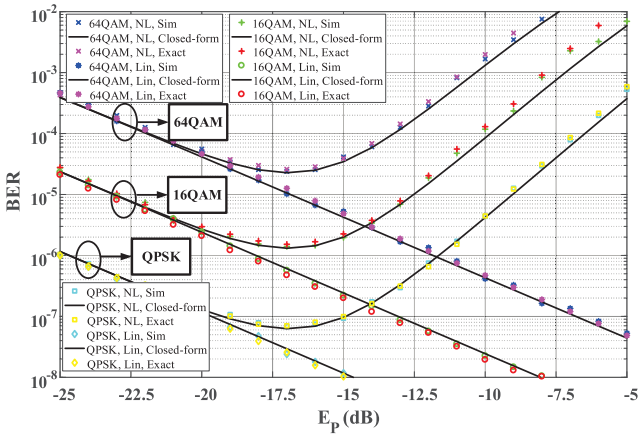

FIGURE 2. The analytical and simulated results of BER as the functions of E_P as three signal modulation schemes applied. Both nonlinear and linear power amplifiers are considered. $X_T = 2$, $X_R = 1$, $\sigma_e^2 = -70dB$, $\sigma_{ch}^2 = -50dB$, $K = 0$ and $\Delta = 0$.

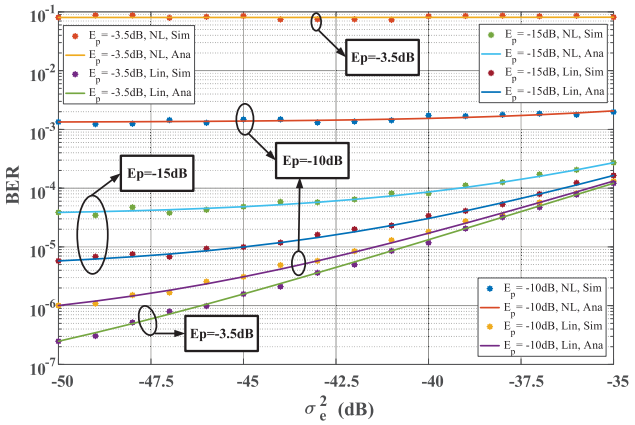

FIGURE 4. The analytical and simulated results of BER as the functions of σ_e^2. Both nonlinear and linear power amplifiers are considered; $X_T = 2$, $X_R = 1$, $E_P = -3.5/-10/-15dB$, $\sigma_{ch}^2 = -50dB$, $K = 0$ and $\Delta = 0$.

be seen that the results of using closed formulas are very close to those obtained using exact expressions and simulation results.

Fig.3 presents both simulated and analytical BER as function of σ_e^2. It can be seen that, BER gets into saturation when σ_e^2 is tiny enough for the cases of nonlinear power amplifiers. This is because, when σ_e^2 is neglectable, we can have that $\gamma_{dec} = \gamma_{dec}^{Lin}$. Thus, based on eq.(39) and eq.(45), it can be derived that here BER is independent with σ_e^2. Also, it is interesting to find that, $\partial BER/\partial E_P > 0$ as σ_e^2 gets small enough, while $\partial BER/\partial E_P < 0$ as σ_e^2 gets large enough. This is because that $\gamma_{dec} = \gamma_{dec}^{Lin}$ and $\gamma_{dec} = \gamma_{dec}^{Nlin}$ when σ_e^2 gets small and big enough, respectively.

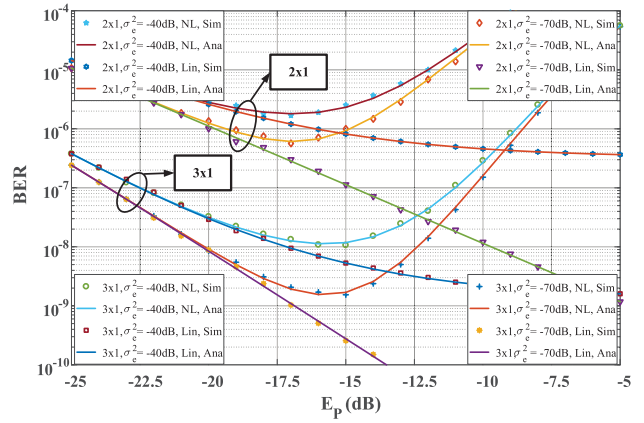

FIGURE 3. The analytical and simulated results of BER as the functions of E_P as applying various MIMO structures. Both nonlinear and linear power amplifiers are considered; $X_T = 2/3$, $X_R = 1$, $\sigma_e^2 = -70/-40dB$, $\sigma_{ch}^2 = -50dB$, $K = 10$ and $\Delta = 1$.

Fig.4 presents the simulated and analytical BER as the functions of E_P as applying various MIMO structures. As expected, E_{P-best} can be identified when nonlinear power amplifiers are applied. BER decreases as either X_R or X_T gets increased for the cases of linear PAs, and BER of the 3×1 structure is lower than that of the 2×1 one. As shown in eq.(53), as the power of the input PA decreases, γ_{dec} begins to increase. γ_{dec} gets increased as X_T increases because the increase of X_T decreases the input power of each PA.

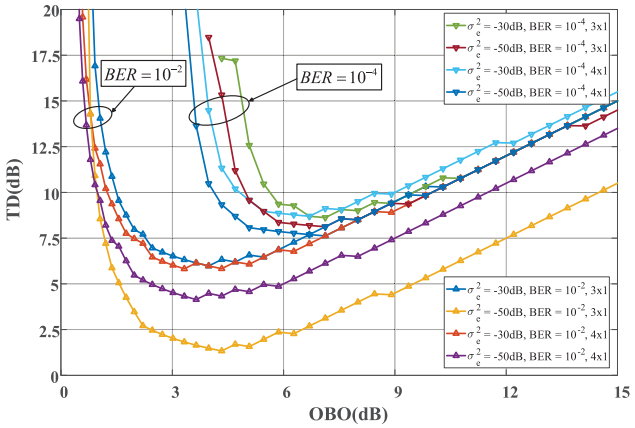

FIGURE 5. The total degradation performance as various target BERs are applied while considering nonlinear PA. The channel estimation error $\sigma_e^2 = -30/-50dB$, $X_T = 3/4$, $X_R = 1$, $K = 10$ and $\Delta = 1$.

Fig.5 presents the TD performance of example nonlinear SFBC MIMO-OFDM system. The x-axis is OBO, i.e., the PA output backoff referring to its maximum output power. It is observed that when the nonlinear power amplifier is operating in its highly nonlinear region, the TD pattern deviates significantly from the graph produced by the linear power amplifier. As shown in Fig.4, when the system damage σ_e^2 can be ignored, the BER will enter a lower saturation, and as the OBO decreases, the lower BER saturation value increases. The BER is in the low value OBO range. At some point of the truncation, the saturation value at the BER associated with the truncation point is equal to the target BER. It can be understood that when the TD cutoff point occurs, the OBO value at

which the TD cutoff point occurs increases. The target BER is reduced. This can be observed in Fig.4 and Fig.5.

Fig.6 presents the analytical and simulated channel capacity as the function of OBO with QPSK scheme. As expected, while considering nonlinear PA, nonlinear distortion is slight when OBO is low. Moreover, the optimal system output back off OBO^{best} corresponding to the channel capacity upper bound can be identified.

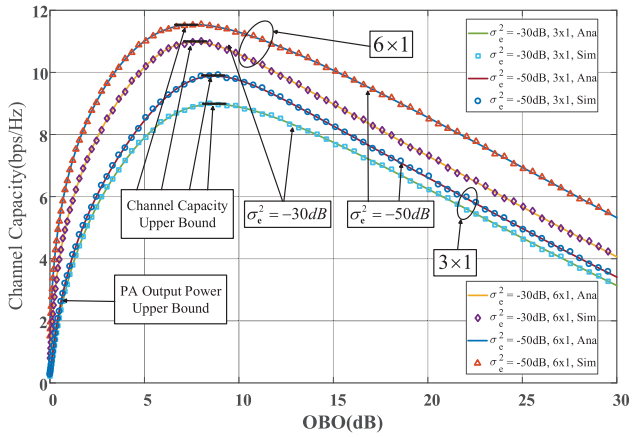

FIGURE 6. The analytical and simulated result of channel capacity as the function of Output Back Off (OBO) while considering nonlinear power amplifiers. The channel estimation error $\sigma_e^2 = -30/-50dB$, $X_T = 4/6$, $X_R = 1$, $\sigma_{ch}^2 = -50dB$, $K = 10$ and $\Delta = 1$.

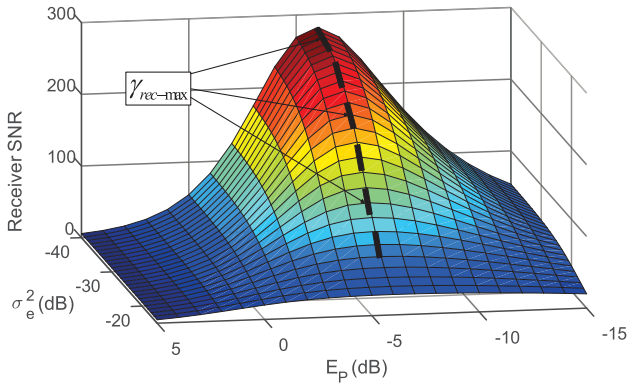

FIGURE 7. The analytical results of receiver SNR γ as the function of the channel estimation error σ_e^2 and the system optimal operating point E_P. Nonlinear PA is considered.

Fig.7 presents the analytical results of receiver SNR γ_{rec} as the function of system operating point E_P and the channel estimation error σ_e^2 roughly. The upper bound of γ, $\gamma_{rec-\max}$ is marked. As expected, receiver SNR γ_{rec} is negatively related to channel estimation error σ_e^2. System optimal operating point E_{P-best} is positively related to channel estimation error σ_e^2.

Fig.8 presents the analytical results of channel capacity C as the function of system operating point E_P and the channel estimation error σ_e^2 roughly. The upper bound of C, $C_{\max}$

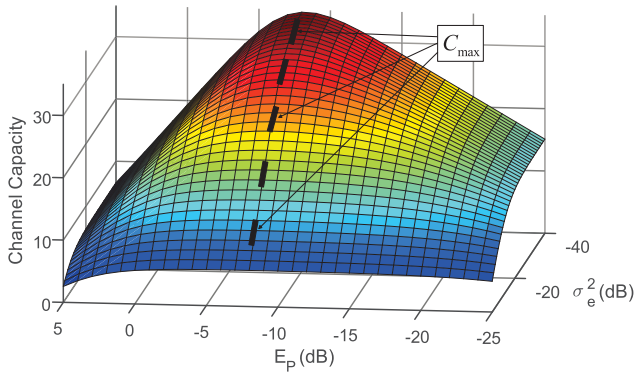

FIGURE 8. The analytical results of channel capacity C as the function of system operating point E_P and the channel estimation error σ_e^2. Nonlinear PA is considered.

is marked. As expected, channel capacity C is negatively related to channel estimation error σ_e^2.

VII. CONCLUSION

In this paper, the performance of SFBC MIMO-OFDM system in the presence of clear nonlinear distortion over TWDP fading channel with imperfect CSI is analyzed. Considering the channel estimation error, we study the lower and upper bounds of mutual information. Furthermore, based on inter modulation product analysis, the receiver SNR is derived as a polynomial function of the system operating point, and its asymptotic behavior is also derived for the cases of linear and nonlinear power amplifiers are considered. Based on these efforts, the optimal system operating point corresponding to the BER lower bound can be identified and analytically derived to a polynomial-based function. In the following, the bit error rate of the PSK and QAM signals is derived. Through these derivations, the observations supporting the simulation are analyzed and explained. The proposed closed-form expressions can be used to quantify the amount of degradation that the BER suffers with nonlinear distortion under imperfect CSI at the receiver, and to devise adaptive link adaptation techniques.

ACKNOWLEDGMENT

(Yipeng Du and Jian Liu are co-first authors.)

REFERENCES

[1] T. Nguyen, M. D. Thieu, and Y. M. Jang, "2D-OFDM for optical camera communication: Principle and implementation," *IEEE Access*, vol. 7, pp. 29405–29424, 2019.

[2] A. M. Jaradat, J. M. Hamamreh, and H. Arslan, "Modulation options for OFDM-based waveforms: Classification, comparison, and future directions," *IEEE Access*, vol. 7, pp. 17263–17278, 2019.

[3] S. S. Ali, D. Castanheira, A. Alsohaily, E. S. Sousa, A. Silva, and A. Gameiro, "Joint space-frequency block codes and signal alignment for heterogeneous networks," *IEEE Access*, vol. 6, pp. 71099–71109, 2018.

[4] M. Gao, Y. Li, O. A. Dobre, and N. Al-Dhahir, "Blind identification of SFBC-OFDM signals using subspace decompositions and random matrix theory," *IEEE Trans. Veh. Technol.*, vol. 67, no. 10, pp. 9619–9630, Mar. 2018.

[5] M. Marey and O. A. Dobre, "Automatic identification of space-frequency block coding for OFDM systems," *IEEE Trans. Wireless Commun.*, vol. 16, no. 1, pp. 117–128, Jan. 2017.
[6] M. Marey, "Integer CFO estimation algorithm for SFBC-OFDM systems," *IEEE Commun. Lett.*, vol. 22, no. 8, pp. 1632–1635, Aug. 2018.
[7] K.-C. Chan, Y.-M. Chen, C.-J. Wu, and C.-P. Li, "Achieving full diversity on a single-carrier distributed QOSFBC transmission scheme utilizing PAPR reduction," *IEEE Trans. Commun.*, vol. 66, no. 4, pp. 1636–1648, Apr. 2018.
[8] W.-W. Hu, W.-J. Huang, Y.-C. Ciou, and C.-P. Li, "Reduction of PAPR without side information for SFBC MIMO-OFDM systems," *IEEE Trans. Broadcast.*, vol. 65, no. 2, pp. 316–325, Jun. 2019.
[9] S.-J. Ku, "Low-complexity PTS-based schemes for PAPR reduction in SFBC MIMO-OFDM systems," *IEEE Trans. Broadcast.*, vol. 60, no. 4, pp. 650–658, Dec. 2014.
[10] J. Han and G. Leus, "Space-time and space-frequency block coded vector OFDM modulation," *IEEE Commun. Lett.*, vol. 21, no. 1, pp. 204–207, Jan. 2017.
[11] F. Delestre, G. Owojaiye, and Y. Sun, "Efficient space–frequency block coded pilot-aided channel estimation method for multiple-input–multiple-output orthogonal frequency division multiplexing systems over mobile frequency-selective fading channels," *IET Commun.*, vol. 8, no. 6, pp. 841–851, Apr. 2014.
[12] H. El Gamal, A. R. Hammons, Jr., Y. Liu, M. P. Fitz, and O. Y. Takeshita, "On the design of space-time and space-frequency codes for MIMO frequency-selective fading channels," *IEEE Trans. Inf. Theory*, vol. 49, no. 9, pp. 2277–2292, Sep. 2003.
[13] M. Torabi, S. Aissa, and M. R. Soleymani, "On the BER performance of space-frequency block coded OFDM systems in fading MIMO channels," *IEEE Trans. Wireless Commun.*, vol. 6, no. 4, pp. 1366–1373, Apr. 2007.
[14] D. Singh and H. D. Joshi, "BER performance of SFBC OFDM system over TWDP fading channel," *IEEE Commun. Lett.*, vol. 20, no. 12, pp. 2426–2429, Dec. 2016.
[15] D. Singh and H. D. Joshi, "Performance analysis of SFBC-OFDM system with channel estimation error over generalized fading channels," *Trans. Emerg. Telecommun. Technol.*, vol. 29, no. 3, p. e3293, Mar. 2018.
[16] D. Singh and H. D. Joshi, "Error probability analysis of STBC-OFDM systems with CFO and imperfect CSI over generalized fading channels," *Int. J. Electron. Commun.*, vol. 98, pp. 156–163, Jan. 2018.
[17] C. van den Bos, M. H. L. Ksuwenhoven, and W. A. Serdijn, "Effect of smooth nonlinear distortion on OFDM symbol error rate," *IEEE Trans. Commun.*, vol. 49, no. 9, pp. 1510–1514, Sep. 2001.
[18] J. Qi and S. Aïssa, "Analysis and compensation of power amplifier nonlinearity in MIMO transmit diversity systems," *IEEE Trans. Veh. Technol.*, vol. 59, no. 6, pp. 2921–2931, Jul. 2010.
[19] P. Banelli and S. Cacopardi, "Theoretical analysis and performance of OFDM signals in nonlinear AWGN channels," *IEEE Trans. Commun.*, vol. 48, no. 3, pp. 430–441, Mar. 2000.
[20] G. D. Durgin, T. S. Rappaport, and D. A. de Wolf, "New analytical models and probability density functions for fading in wireless communications," *IEEE Trans. Commun.*, vol. 50, no. 6, pp. 1005–1015, Jun. 2002.
[21] M. Rao, F. J. Lopez-Martinez, M. S. Alouini, and A. Goldsmith, "MGF approach to the analysis of generalized two-ray fading models," *IEEE Trans. Wireless Commun.*, vol. 14, no. 5, pp. 2548–2561, May 2015.
[22] H. S. Kim and B. Daneshrad, "Power optimized PA clipping for MIMO-OFDM systems," *IEEE Trans. Wireless Commun.*, vol. 10, no. 9, pp. 2823–2828, Sep. 2011.
[23] N. S. O'Droma and N. Mgebrishvili, "Signal modeling classes for linearized OFDM SSPA behavioral analysis," *IEEE Commun. Lett.*, vol. 9, no. 2, pp. 127–129, Feb. 2005.
[24] H. Shin and J. H. Lee, "Performance analysis of space-time block codes over keyhole Nakagami-m fading channels," *IEEE Trans. Veh. Technol.*, vol. 53, no. 2, pp. 351–362, Mar. 2004.
[25] A. Maaref and S. Aissa, "Capacity of space-time block codes in MIMO Rayleigh fading channels with adaptive transmission and estimation errors," *IEEE Trans. Wireless Commun.*, vol. 4, no. 5, pp. 2568–2578, Sep. 2005.
[26] L. H. Ozarow, S. Shamai (Shitz), and A. D. Wyner, "Information theoretic considerations for cellular mobile radio," *IEEE Trans. Veh. Technol.*, vol. 43, no. 2, pp. 359–378, May 1994.
[27] M. S. O'Droma, "Dynamic range and other fundamentals of the complex Bessel function series approximation model for memoryless nonlinear devices," *IEEE Trans. Commun.*, vol. 37, no. 4, pp. 397–398, Apr. 1989.
[28] X.-G. Xia, "Precoded and vector OFDM robust to channel spectral nulls and with reduced cyclic prefix length in single transmit antenna systems," *IEEE Trans. Commun.*, vol. 49, no. 8, pp. 1363–1374, Aug. 2001.
[29] S. T. Chung and A. J. Goldsmith, "Degrees of freedom in adaptive modulation: A unified view," *IEEE Trans. Commun.*, vol. 49, no. 9, pp. 1561–1571, Sep. 2001.

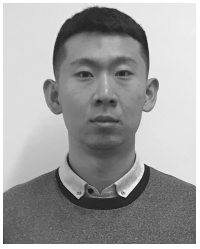

YIPENG DU received the B.Sc. degree in communication engineering from the University of Science and Technology Beijing, Beijing, China, in 2018. He is currently pursuing the M.S. degree with the School of Electronics Engineering and Computer Science, Peking University, Beijing. His current research interests include performance analysis to nonlinear wireless transmitter systems, natural language processing, and computational modeling and simulation of tumor treating fields.

JIAN LIU (M'09) received the B.S. degree in automatic control theory and applications from Shandong University, China, in 2000, and the Ph.D. degree from the School of Information Science and Engineering, Shandong University, in 2008. He is currently an Associate Professor with the University of Science and Technology Beijing, China. His research interests include cognitive radio networks, mobile mesh networks, and key technology of next generation wireless communication systems.

YUAN CHEN was born in Shandong, China. She received the B.Sc. degree from the School of Information Science and Engineering, Shandong University, in 2010, and the Ph.D. degree in electronic engineering from the City University of Hong Kong, in 2015. Since 2015, she has been with the School of Computer and Communication Engineering, University of Science and Technology Beijing, where she is currently an Assistant Professor. Her research interests include statistical signal processing, frequency estimation, machine learning, and their applications.